NMR relaxation study of the H-bonded glass $Rb_{1-x}(NH_4)_xH_2PO_4$

J. Slak,* R. Kind, and R. Blinc*
Laboratory of Solid State Physics, Swiss Federal Institute of Technology, ETH-Hönggerberg, CH-8093 Zurich, Switzerland

Eric Courtens
IBM Zurich Research Laboratory, CH-8803 Rüschlikon, Switzerland

S. Žumer
Department of Physics, E. Kardelj University of Ljubljana, 61001 Ljubljana, Yugoslavia
(Received 5 December 1983)

The existence of a minimum in the temperature dependence of the ^{87}Rb spin-lattice relaxation time T_1 in $Rb_{1-x}(NH_4)_xH_2PO_4$ with $x=0.35$ indicates a tremendous progressive slowing down of the proton intrabond (O—H $\cdots$ O) jump motion from $\sim 10^{-11}$ to $\sim 10^{-7}$ sec not found in RbH_2PO_4 or other members of the KH_2PO_4 family exhibiting ferro- or antiferroelectric transitions. The occurrence of a linewidth broadening together with the T_1 minimum exhibits a wide distribution of correlation times that develops near the onset of the low-frequency dielectric dispersion and loss characteristic of the glass state. The results can be described in terms of a cluster freeze-out model originally developed for spin-glasses. The NH_4 reorientations freeze out much before the low-temperature glass state has been reached.

I. INTRODUCTION

Magnetic systems with random competing interactions often exhibit a spin-glass state.[1] It is still not clear whether the freezing of spins, or clusters of spins, into random orientations is a local nonequilibrium dynamic process or a real equilibrium phase transition with an infinite correlation length below a well-defined critical temperature T_G. Recently, a hydrogen-bonded analog of such systems has been found, in which ferroelectric RbH_2PO_4 and antiferroelectric $NH_4H_2PO_4$ constituents are mixed.[2] Dielectric and birefringence data indicated that for $x<0.22$ the ferroelectric transition still occurs in mixed crystals of $Rb_{1-x}(NH_4)_xH_2PO_4$, whereas for $x>0.8$ the antiferroelectric transition appears.[3] However, in the range $0.22<x<0.8$, these structural changes are not found; rather, the crystals freeze into random configurations resembling magnetic spin-glasses.[3] A tentative phase diagram for such mixed systems was recently evaluated in the cluster approximation, and stability limits for the ferroelectric, spin-glass, and antiferroelectric phases were discussed.[4] It should be noted that in this system, the interactions are not simply of the Ising or Heisenberg type, but that Slater rules[5] must be taken into account, whereby the six lowest-energy configurations are the ones with only two acid protons "close" to each PO_4 group. The ferroelectric ground state is characterized by "up-down" H_2PO_4 configurations, and the antiferroelectric one by "lateral" configurations. In the mixed system, the configurations are expected to vary randomly throughout the crystal.

In order to clarify the local dynamics of this system, we measured the ^{87}Rb and ^1H spin-lattice relaxation rate as a function of temperature in a $Rb_{1-x}(NH_4)_xH_2PO_4$ single crystal with $x=0.35$, a concentration where the tetragonal-to-orthorhombic ferroelectric transition is suppressed and replaced by glass behavior. Specifically, at that concentration, a first set of anomalies suggesting progressive freezing, presumably first related to the ammonia sites, develops below ~ 100 K.[3,6] This evolves into a compressibility anomaly near 50 K,[6] and into low-frequency dielectric dispersion and loss whose onset at 1 kHz is near 30 K.[3,7] Furthermore, the dielectric measurements are well explained with a Vogel-Fulcher freezing temperature of 10 K.[7] In view of the richness of these phenomena the definition of a glass transition temperature would be so far rather arbitrary. It should be noted that the system still rearranges itself at temperatures much lower than the ordering transition of the pure crystals (~ 150 K).[3]

II. EXPERIMENTAL METHOD

The spectrometer, operating at a frequency of $\nu_L=30.780$ MHz, was tuned with RbH_2PO_4, and the dependence of the ^{87}Rb $I_z=\frac{1}{2}\rightarrow I_z-\frac{1}{2}$ line shape and intensity was first measured as a function of the angle between the tetragonal $\vec{c}$ axis and the applied magnetic field $\vec{H}_0$, with $\vec{a}\perp\vec{H}_0$. The signal was strongest with $\vec{c}\,||\vec{H}_0$ and $\vec{c}\perp\vec{H}_0$, and broader in between. This effect was much more pronounced for the mixed crystal, in which Rb signals could be measured only around $\vec{c}\,||\vec{H}_0$ and $\vec{c}\perp\vec{H}_0$ at room temperature. Below ~ 100 K, the angular dependence of the Rb frequency seemed to vanish, and a good signal could be obtained only with $\vec{c}\,||\vec{H}_0$. The temperature dependence of the ^1H and ^{87}Rb $I_z=\frac{1}{2}\rightarrow I_z-\frac{1}{2}$ spin-lattice relaxation rates was then studied with $\vec{c}\,||\vec{H}_0$. A 90°-90° pulse sequence with a 90° pulse length of 7 μsec for ^{87}Rb and a Fourier-transform technique were used. There were at least two components in

the proton recovery, and the Rb recovery was not quite exponential either. The line shape will be the subject of a separate study.

III. RESULTS

Similar to pure $NH_4H_2PO_4$ (Ref. 8) or to lightly-NH_4-doped RbH_2PO_4 (Ref. 9), the proton T_1 is dominated by the slow NH_4 reorientations. As with these systems, one finds a broad T_1 minimum near 175 K (Fig. 1). From 300 K down to ~ 120 K, the behavior is well fitted with a Bloembergen-Purcell-Pound-type (BPP) expression[10] and a thermally activated $\tau=\tau_0\exp(E_a/k_BT)$ (Fig. 2). One finds $E_a=3.2$ kcal/mol, $\tau_0=1.8\times10^{-13}$ sec, and a T_1 minimum of ~ 20 msec, in very good agreement with literature values.[8] The lowest-temperature point shown in Fig. 2 ($T=76$ K) emphasizes that the BPP fit does not extend below ~ 100 K, although it extends to at least 77 K in the case of pure $NH_4H_2PO_4$.[8] Other measurements suggest that below ~ 100 K, a progressive freezing of Slater configurations associated with NH_4 groups occurs.[3,6] The departure from the BPP behavior could thus be related to a broad distribution of relaxation times developing in that region of temperature, although T_1 values longer than ~ 1 sec could also be easily affected by unknown paramagnetic impurities. In any case, the reorientation of the NH_4 groups is likely to become so slow near 30 K that it should not play a significant role in the transition to the low-temperature glass state.

The situation is rather different for the ^{87}Rb NMR signal and T_1. At room temperature, the angular dependence of the Rb $I_z=\frac{1}{2}\rightarrow I_z-\frac{1}{2}$ transitions agrees with that in pure RbH_2PO_4 [Fig. 3(a)]. The signal is strong at those orientations where the second-order quadrupole shift of the central line is small (e.g., at $\vec{c}\,||\vec{H}_0$), whereas the line is significantly broadened at other orientations. Below ~ 100 K this broadening becomes so pronounced [Fig. 3(b)] that only the component with zero second-order quadrupole shift could be effectively used for T_1 measurements. Instead of the well-defined angular dependence of the Rb lines as in RbH_2PO_4 [Fig. 3(a)] one then finds a continuous distribution of Rb resonance frequencies in the interval between the maximum and minimum shifts. The distribution is centered at $\nu-\nu_L=0$, resulting in a strong angular dependence of the intensity and half-width of the line [Fig. 3(b)]. It is interesting to note that this broadening starts near 100 K, i.e., in the same region of temperature where anomalies such as deviations from the Curie-Weiss law in the dielectric constant at 1 kHz also become significant.[2,3]

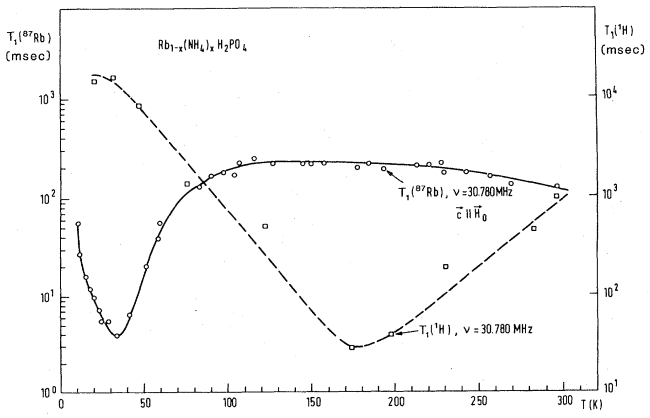

FIG. 1. Temperature dependence of the ^{1}H and ^{87}Rb $I_z=\frac{1}{2}\rightarrow I_z-\frac{1}{2}$ spin-lattice relaxation times in $Rb_{1-x}(NH_4)_xH_2PO_4$ at $\nu_L=30.78$ MHz and with $\vec{c}\,||\vec{H}_0$.

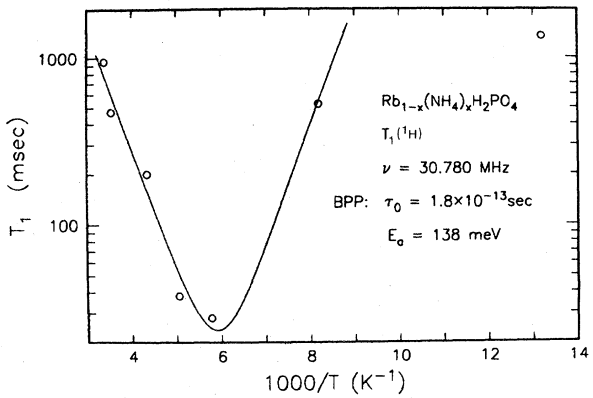

FIG. 2. Semilogarithmic plot of T_1 vs $10^3/T$ for the proton spin-lattice relaxation time. The solid line is a BPP fit of the six highest temperature points.

The average ^{87}Rb spin-lattice relaxation time (Fig. 1) was obtained by fitting the observed magnetization recovery to a single effective exponential curve, thus neglecting the very fast and very slow relaxation components. It slowly increases with decreasing temperature from 300 K to about 115 K. This suggests that it is mostly controlled in this interval by a motion which is slow compared to the nuclear Larmor frequency ($\omega_L\tau_{c1}\gg 1$). In analogy with other KH_2PO_4-type systems,[11] one tentatively assigns the process to slow proton interbond jumps[12] caused by 90° reorientations of the H_2PO_4 groups. It should be noted, however, that the slope of the $\log T_1$-versus-$1/T$ plot (Fig. 4) gives an activation energy of about 20 meV for $300>T>150$ K, while the temperature dependence of the electrical conductivity gives ~ 670 meV for the range $300>T>220$ K.[13]

Below 115 K, the ^{87}Rb spin-lattice relaxation time starts to decrease with increasing temperature, indicating that a new fast ($\omega_L\tau_{c2}\ll 1$) motional process becomes active. In analogy with other KH_2PO_4 systems, we can ascribe this effect to proton intrabond jumps.[12] This motion leads to a switching between the 16 possible proton configurations around a given PO_4 group.[14] The decrease in T_1 apparently follows a simple thermally activated motional process down to $T\simeq 35$ K where a T_1 minimum is found. In the simplest model, the T_1 minimum occurs when the average proton intrabond jump rate becomes of the order of the nuclear Larmor frequency, i.e.,

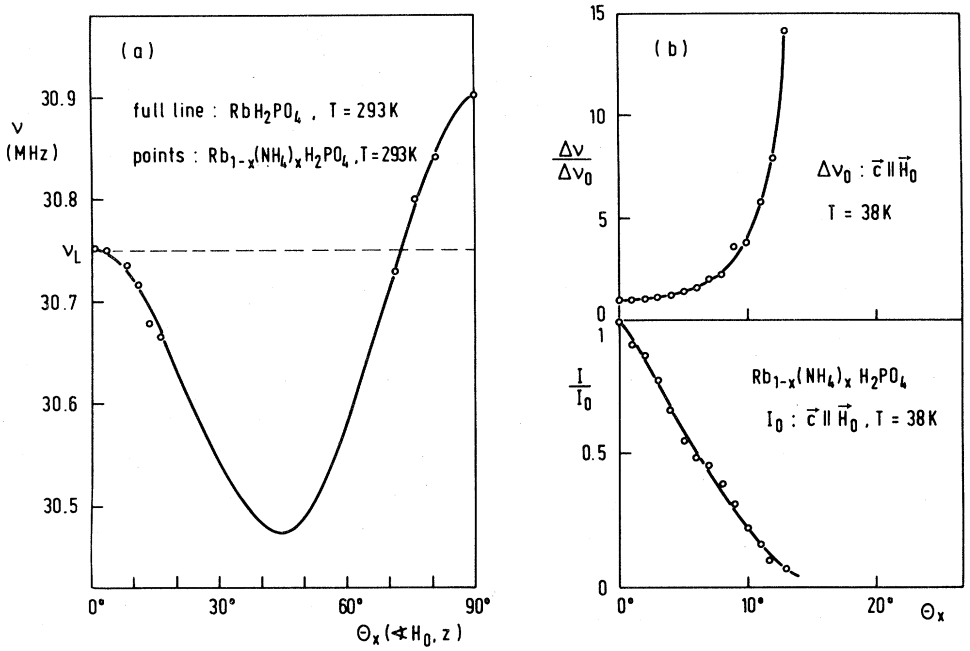

FIG. 3. (a) Angular dependence of the second-order quadrupole shifts of the Rb $I_z=\frac{1}{2}\rightarrow I_z=-\frac{1}{2}$ line in RbH_2PO_4 and in $Rb_{1-x}(NH_4)_xH_2PO_4$. (b) Angular dependence of the peak intensity and half-width of the Rb lines in $Rb_{1-x}(NH_4)_xH_2PO_4$. The half-widths are only rough estimates. In pure RbH_2PO_4, the Rb half-width is practically independent of angle.

$\tau_{c2}\simeq 0.6\times 10^{-8}$ sec. Below the minimum, T_1 increases with decreasing temperature down to the lowest measured value, ~ 10 K. In this slow-motion regime, a semilogarithmic plot of T_1 versus $1/T$ (Fig. 4) reveals that the rate-determining motion can no longer be described as thermally activated with a temperature-independent activation energy.

IV. DISCUSSION

The ^{87}Rb NMR and relaxation in the mixed crystal with $x=0.35$ exhibits a number of features which are absent in pure RbH_2PO_4:

(a) The recovery of the nonequilibrium magnetization is nonexponential, demonstrating the existence of relaxation times that can be related to a spatial inhomogeneity resulting from a cluster distribution.

(b) The decrease of T_1 with decreasing temperature which requires $\omega_L\tau_{c2}\ll 1$ is accompanied by an anamolous broadening of the linewidth requiring $\omega_L\tau_{c2}>1$. This suggests that the distribution of τ_{c2} extends all the way from less than 10^{-10} to 10^{-3} sec and more.

(c) The existence of a T_1 minimum in the region of onset of dielectric losses implies a tremendous slowing down of the proton intrabond (O—H $\cdots$ O) switching motion, from 10^{-11} to more than 10^{-8} sec, a phenomenon so far not observed for any KH_2PO_4-type crystal exhibiting either a paraelectric-to-ferroelectric or a paraelectric-to-antiferroelectric transition.

(d) The transition to the dynamic glass state below 30 K is *not* accompanied by an observable power-law anomaly of the relaxation time, as it usually is in ordinary paraelectric-to-ferroelectric transitions where the critical correlation time $\tau_{q_{\rm crit}}$ diverges at the transition temperature T_c. It is, however, connected with a further slowing down of the proton intrabond motion and with the onset of a temperature dependence of the apparent activation energy for this motion.

The features listed above are distinct from what is observed at usual equilibrium phase transitions. They appear compatible with a dynamical description of the glass formation. It would then be connected with a freeze out of weakly interacting clusters of H_2PO_4 groups, or of quasilocal modes, of variable spatial extent. Each unit would relax with a correlation time $\tau_{c2}=\tau_{c2}(\xi)$, where $\xi(T)$ is its characteristic size.

A. Spin relaxation

Putting these statements onto a more quantitative basis, the ^{87}Rb($I=\frac{3}{2}$) spin-lattice relaxation process in a high magnetic field ($\nu_L\gg\nu_Q$) at a general orientation is characterized by the rates $2W_1$ and $2W_2$, where

$$W_k=\frac{e^4Q^2}{8I\hbar^2}J^{(k)}(k\omega)\,, \tag{1}$$

with

$$J^{(k)}(\omega)=\int_{-\infty}^{+\infty}\langle V_{(k)}(0)V_{(-k)}(t)\rangle e^{i\omega t}dt \tag{2}$$

representing the spectral density of the autocorrelation function of the fluctuating part of the Rb electric-field-gradient (EFG) tensor components $V_{(k)}$ expressed in the magnetic-field-fixed laboratory frame. Assuming that the EFG tensors on Rb sites maintain the strong anisotropy of the pure system ($x=0$), one can write $1/T_1=2W_2$ for the present field orientation.[15]

The time dependence of the Rb EFG tensor can be expanded to

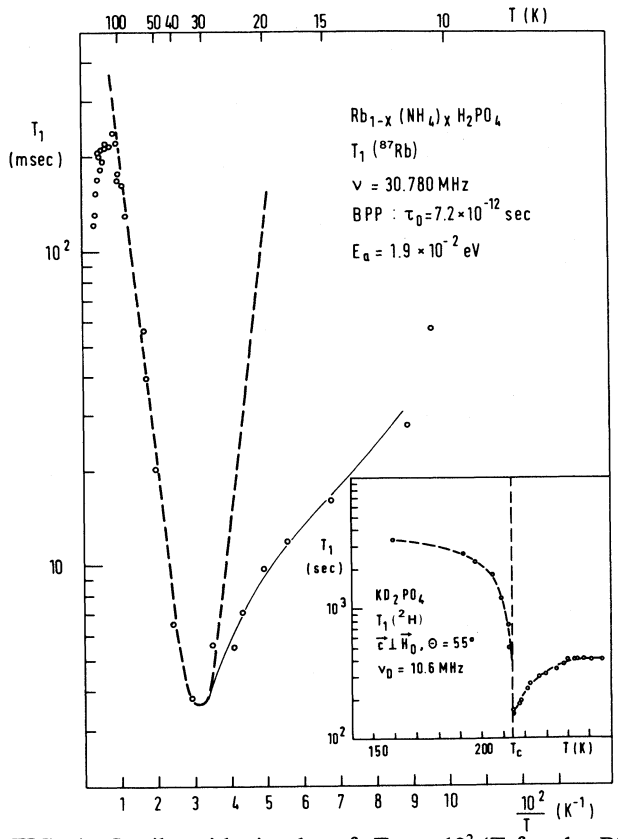

FIG. 4. Semilogarithmic plot of T_1 vs $10^2/T$ for the Rb $I_z=\frac{1}{2}\rightarrow I_z=-\frac{1}{2}$ spin-lattice relaxation time. The dashed line shows the dependence predicted by a BPP expression with a thermally activated correlation time and a constant activation energy. The solid line is a guide to the eye. The inset shows the temperature dependence of the deuterium T_1 in KD_2PO_4 for comparison.

$$V(t)=V_0+\sum_i A_i p_i(t)+\cdots\ , \tag{3}$$

where p_i is the local order parameter of an elementary reversible O—H $\cdots$ O dipole that fluctuates between $+1$ and -1. The summation extends over all neighboring O—H $\cdots$ O bonds that still give a nonvanishing contribution to the Rb EFG tensor. Expression (3) is thus related to the local spectral density of the order-parameter fluctuations

$$J^{(k)}(\omega)=\int_{-\infty}^{+\infty}\left\langle\sum_{i,j}A_j^{(k)}A_j^{(-k)}p_i(0)p_j(t)\right\rangle e^{i\omega t}dt\ . \tag{4}$$

When dealing with an ordinary phase transition, collective coordinates $p_{\vec{q}}(t)$ are introduced as Fourier components of $p_i(t)$. Via the fluctuation-dissipation theorem, $J^{(k)}(\omega)$ is related to the imaginary part of the wave-number-dependent dynamic susceptibility $\chi(\vec{q},\omega)$:

$$J^{(k)}(\omega)\propto\frac{1}{\omega}\sum_{\vec{q}}\chi''(\vec{q},\omega)\ , \tag{5}$$

where

$$\chi''(\vec{q},\omega)=\chi(\vec{q},0)\frac{\omega\tau_{\vec{q}}}{1+\omega^2\tau_{\vec{q}}^2} \tag{6a}$$

and

$$\tau_{\vec{q}}\propto\chi(\vec{q},0)\tau\ , \tag{6b}$$

with $\tau(\vec{q}_c,0)$ diverging at T_c and with τ standing for the single-particle reorientation time. In all KH_2PO_4-type systems investigated so far, NMR experiments were performed in the fast-motion limit: $\omega_L\tau_{c2}\ll1$ for all $\vec{q}$ in the entire experimentally accessible temperature range. Hence, T_1 usually exhibited a power-law anomaly $T_1\propto|T-T_c|^n$ as T approached T_c.

B. Edwards-Anderson Sherrington-Kirkpatrick model

In the theory of Edwards and Anderson (EA), and in the Sherrington-Kirkpatrick model, there is an equilibrium phase transition to the spin-glass phase.[16] The order parameter of the spin-glass transition is

$$q=\lim_{t\rightarrow\infty}[\langle p_i(0)p_i(t)\rangle]_i\ , \tag{7}$$

where the $[\ ]_i$ designates the average over the sites. Above T_G, q is 0 and behaves as $(T_G-T)/T_G$ below T_G. In mean field,[16] a static local susceptibility χ_{EA} diverges at T_G, which would predict an anomalous power-law behavior of the local dipolar reorientation time τ_{loc} and of T_1, in apparent contradiction to the present observations if T_G were located at the onset of the dielectric losses ($T_G\simeq30$ K).[2]

C. Independent-cluster model

In the "independent-cluster" model[1,17] of the spin-glass phase, where $p_i(t)=\pm p_j(t)$ when both dipoles are in the same cluster, the correlation function consists of a sum of exponentially decaying terms,

$$\langle p_i(0)p_i(t)\rangle=\sum_\alpha P_\alpha^2 e^{-t/\tau_\alpha}\ , \tag{8}$$

where P_α are the amplitudes of the polarization fluctuations corresponding to τ_α which are thermally activated. For the longest correlation time τ_c, the activation energy should depend on the number of particles in the cluster:[17]

$$\tau_c=\tau_0\exp[E_a(\xi)/k_BT]\ . \tag{9}$$

Here ξ is the correlation length which determines the cluster size and varies with temperature. In the independent-cluster model, E_a is proportional to a positive power of $1/T$.[17] For weakly interacting clusters, the Vogel-Fulcher law,

$$\tau=\tau_0\exp[E/k_B(T-T_0)]\ , \tag{10}$$

has been proposed to analyze the ac susceptibility data.[18] A finite temperature T_0 should arise from intercluster coupling.[18] Its value is generally far below the dynamic glass temperature.

At frequencies $\omega<\tau_c^{-1}$, the longest correlation time τ_c dominates the magnetic relaxation so that

$$W_k=\frac{e^4Q^2}{8I\hbar^2}|\mathscr{A}^{(k)}|^2P_c^2\frac{2\tau_c}{1+(k\omega\tau_c)^2} \tag{11}$$

has a BPP form, where $\mathscr{A}^{(k)}=\sum_i A_i^{(k)}$, and P_c is the corresponding amplitude of the polarization fluctuations.

If the experimental data are analyzed with a BPP formula[19] using a single average correlation time and a temperature-independent activation energy, a symmetric T_1-versus-$1/T$ semilogarithmic plot is predicted. Such a plot apparently fits the experimental T_1 data on the high-temperature side of the T_1 minimum with an activation energy $E_a=1.95\times10^{-2}$ eV, but not on the low-temperature side (Fig. 4). Below the T_1 minimum, significant deviations from the BPP expression (11) occur, the curve definitely being nonsymmetric. The apparent activation energy is 6 times smaller on the low-temperature side.

The value of τ_0 derived from the T_1 minimum is $\tau_0=7.2\times10^{-12}$ sec. Using this value in Eq. (10), from the experimental data one evaluates the temperature dependence of a mean effective cluster correlation time τ_{c2} representing the biased mean proton intrabond motion. The result is shown in Fig. 5. The mean τ_{c2} varies from 4×10^{-11} sec at 100 K to 1.5×10^{-8} sec at 27 K. It is of the order of 1.8×10^{-7} sec at 11 K. It must be stressed that these values represent only mean correlation times obtained in the BPP approximation. The simultaneous occurrence of a line broadening and of a T_1 minimum, as well as the deviations of the $\log T_1$-versus-$1/T$ plot from the BPP form, demonstrate the occurrence of a wide distribution in the correlation times τ_{c2}.

In such a case, Eqs. (1) and (2) for the average rates W_1 and W_2 can be written

$$W_k=\frac{1}{12}\frac{e^4Q^2}{\hbar^2}|\mathscr{A}^{(k)}|^2\frac{P_c^2}{k\omega}[D(k\omega\tau)]_f\ , \tag{12}$$

where

$$D(\omega\tau)=\frac{2\omega\tau}{1+\omega^2\tau^2}=\frac{1}{\cosh[\ln(\omega\tau)]}\ , \tag{13a}$$

$$\ln(\omega\tau)=\ln(\omega\tau_0)+E/k_BT\ , \tag{13b}$$

$$[D(\omega\tau)]_f\equiv\int_0^\infty f(x)D(\omega\tau(x))dx\ . \tag{13c}$$

In the above, the Debye-type spectral densities D are averaged over a distribution of activation energies $f(x)$, with $x=E/k_BT$, the distribution being assumed to arise from a distribution of cluster sizes, the correlation time τ being related to the cluster activation energy by Eq. (13b). Here, P_c is taken as a constant. These average rates can be introduced only when magnetic dipolar interactions between clusters ensure a common spin-lattice relaxation. This is not completely realized in the present case as the experimental decay curves are not quite exponential.

Several distributions $f(x)$ could be used to fit the experimental T_1 values. Without additional information, the simplest one-parameter distribution is

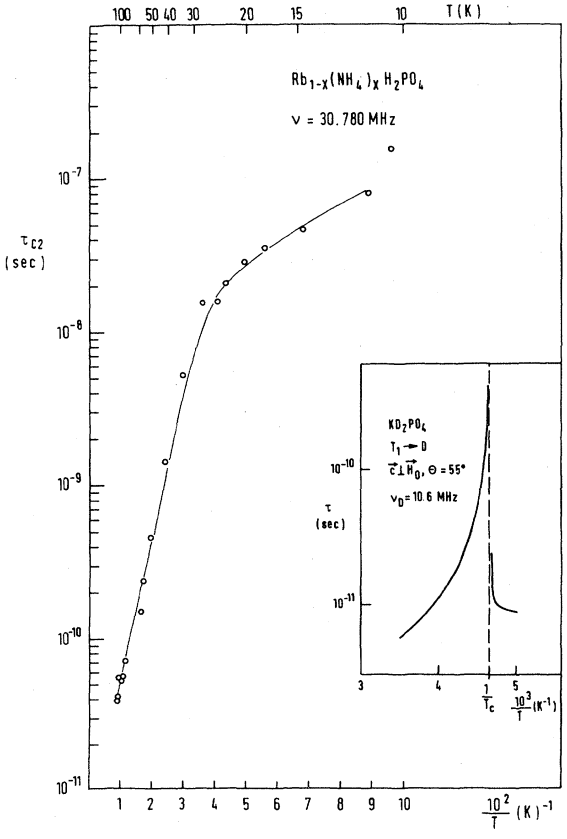

FIG. 5. Temperature dependence of an effective mean proton intrabond jump time τ_{c2} in $Rb_{1-x}(NH_4)_xH_2PO_4$ derived from the Rb T_1 minimum assuming the validity of the BPP approximation. The inset shows the deuteron intrabond correlation time τ in KD_2PO_4 as derived from T_1 data.

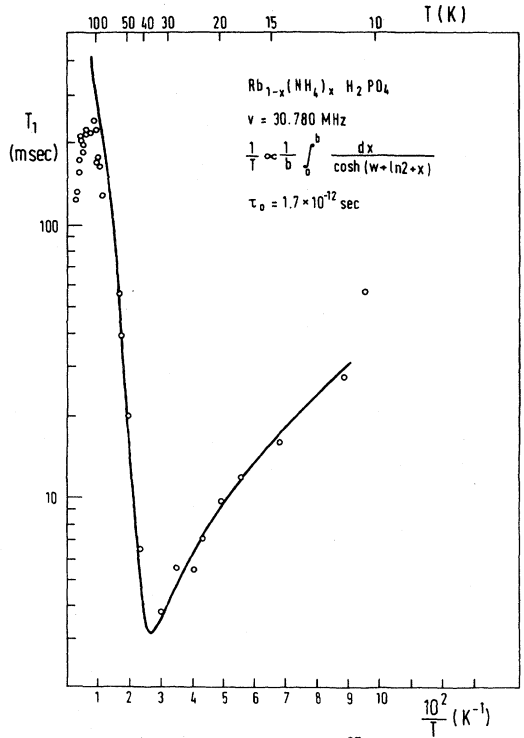

FIG. 6. Fit of the experimental ^{87}Rb T_1 data using a temperature-dependent square distribution of activation energies according to Eqs. (12)—(15).

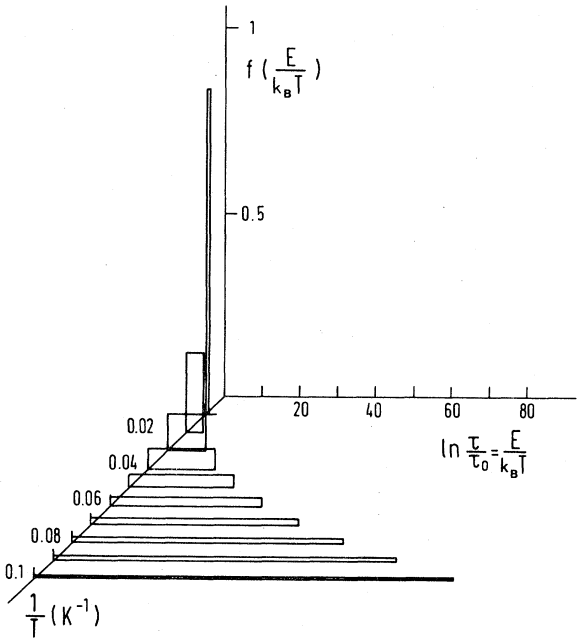

FIG. 7. Variation of the distribution of activation energies $f(E/kT)$ and correlation times $\ln(\tau/\tau_0)$ with temperature, assuming the validity of the distribution Eqs. (14a) and (14b) with $b \propto 1/T^2$ and $E \propto 1/T$.

$$f(x)=\begin{cases}1/b & \text{for } x<b \quad (14a)\\ 0 & \text{for } x>b\ , \quad (14b)\end{cases}$$

i.e., a uniform distribution of activation energies. In this case, using the data of Blinc *et al.*[15] for the ^{87}Rb EFG in RbH_2PO_4, for the present magnetic field orientation one finds the rate

$$\frac{1}{T_1}=2W_2=\frac{1}{12}\frac{e^4Q^2}{\hbar^2}|\mathscr{A}^{(2)}|^2\frac{P_c^2}{b\omega}\int_0^b\frac{dx}{\cosh(w+x+\ln 2)}\ , \quad (15)$$

with $e^2Q\mathscr{A}^{(2)}/\hbar=1.5\times10^7$ sec^{-1}, where $w=\ln(\omega\tau_0)$, and $E_a=bk_BT$. Assuming $E_a\propto 1/T$, i.e., a complete freeze out at $T=0$, $b=\beta/T^2$ follows. The fit between the experimental T_1 and the one predicted by Eq. (15) is rather good (Fig. 6). This fit yields $w=-8$, that is, $\tau_0=1.7\times10^{-12}$ sec, $\beta=1.1\times10^4$ K^2, and $P_c=0.1$. The latter value indicates that only 10% of the polarization fluctuates with the longest correlation time within this model. Also, the spread in activation energies $f(x)$ increases by a factor of 10 between 100 and 10 K, resulting in a tremendous increase in the average cluster correlation time. The corresponding distribution is shown in Fig. 7.

D. Fits with a Vogel-Fulcher law

It should be noted that on the basis of the present NMR data alone, it is not possible to distinguish between different distributions, or between an Arrhenius and a Vogel-Fulcher behavior. A solid test of the distribution would be contained in the frequncy dependence of $[D]_f$, for which NMR data at other frequencies, or $T_{1\rho}$ data, are not yet available. However, a distribution of correlation times was recently derived from audio-frequency measurements of the complete dielectric constant.[7] These measurements demonstrated that the correlation-time distribution is broad in $\ln\tau$ and that it can be derived from a temperature-independent distribution of activation energies E related to the times by the Vogel-Fulcher law, Eq. (10). The audio measurements gave $T_0=10$ K, and $\ln\nu_0=27.83$ where $\nu_0=1/2\pi\tau_0$ is in Hz. The temperature-independent energy distribution is of the form[7]

$$f(E)=\frac{N}{E_c}\tfrac{1}{2}\{1+\tanh[d(E_c-E)]\}\ , \quad (16)$$

where the cutoff energy in temperature units is $E_c=(228\pm3)$ K, $d=0.0134$ K^{-1}, and N is the normalization constant practically equal to 1. Defining a correlation-time distribution $g(\tau,T)$ normalized to 1 when integrated over $d\ln\tau$, one finds[7]

$$g(\tau,T)=(T-T_0)f(E)\ . \quad (17)$$

These energy and time distributions are drawn in Fig. 8.

As the audio measurements covered up to 4 orders of magnitude in frequency, and as the frequency dependence is logarithmic, an upward extrapolation of the distribution by another $2\frac{1}{2}$ orders of magnitude is not unreasonable.

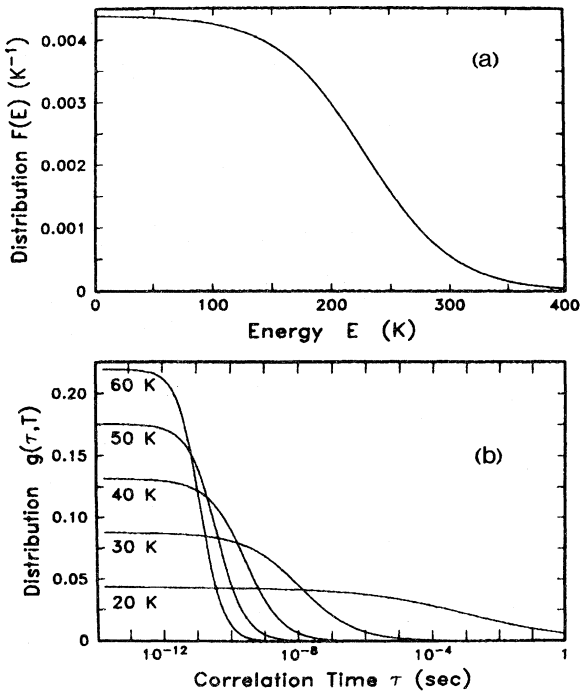

FIG. 8. (a) Distribution of activation energies obtained from dielectric loss measurements in Ref. 18. (b) The corresponding distribution of correlation times for five temperatures above the Vogel-Fulcher temperature $T_0=10$ K.

One then assumes that the same distribution approximately holds for the ^{87}Rb spin-lattice relaxation, which allows evaluation of the corresponding T_1. In the fast-motion regime, one can approximate $g(\tau,T)$ by

$$g=\begin{cases}(T-T_0)/E_c & \text{for } E<E_c \quad (18a)\\ 0 & \text{for } E>E_c\ . \quad (18b)\end{cases}$$

One obtains

$$[D(2\omega_L\tau)]_f=\int_{\tau_0}^{\tau_c}\frac{T-T_0}{E_c}\frac{4\omega_L\tau}{1+(2\omega_L\tau)^2}\frac{d\tau}{\tau}$$
$$\simeq\frac{2(T-T_0)}{E_c}\arctan\frac{2\nu_L}{\nu_c}\ , \quad (19)$$

where $\nu_c=1/2\pi\tau_c$ is related to E_c by Eq. (10), and $\nu_0\ll\nu_L$ was used. Replacing this value of $[D]_f$ in Eq. (12), and using the parameter values given after Eq. (15), one finally has

$$T_1=1/(96.95P_c^2[D]_f)\ , \quad (20)$$

where T_1 is in msec and $[D]_f$ is given by Eq. (19). A good fit to the T_1 values with $120>T>40$ K is obtained by mere adjustment of the parameter P_c. One finds $P_c=0.33$. A slightly better fit results when the value E_c is also allowed to vary. One then obtains $P_c=0.35$ and $E_c=(215\pm9)$ K, which is in remarkable agreement with the E_c value derived from the dielectric data. This fit is presented in Fig. 9. One could also argue that the dielectric relaxation being dipolar and the NMR relaxation being quadrupolar, there might be a scale factor between dielectric and NMR correlation times $\tau_{\text{diel}}\simeq3\tau_{\text{NMR}}$. In this case, one simply replaces ν_L by $\nu_L/3$ in the argument

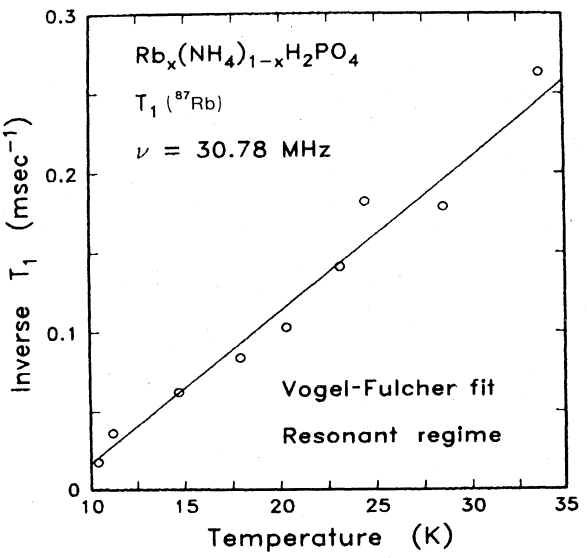

FIG. 9. Experimental Rb T_1 data in the fast-motion regime fitted using a simplified version of the distributions of Fig. 8(b) as explained in the text. The solid line is the best fit with $P_c=0.35$ and $E_c=215$ K.

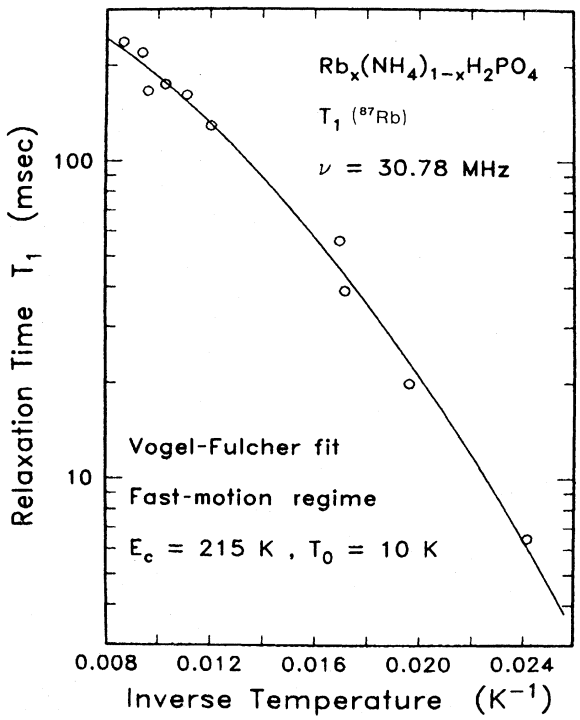

FIG. 10. Experimental Rb relaxation rates in the low-temperature regime fitted to the law $1/T_1\propto T-T_0$. Here, part of the distributions of Fig. 9(b) is nearly resonant at the Larmor frequency.

of the arctan in Eq. (19). This gives no noticeable change of the fit except that $P_c=0.60$ with the same E_c.

As the temperature is lowered below ~40 K, a change of behavior is observed. Part of the distribution $g(\tau,T)$ becomes resonant with the Larmor frequency. The amplitude of this resonant contribution being proportional to $T-T_0$, one expects $T_1^{-1}\propto T-T_0$. This is actually found, as shown in Fig. 10 for the points measured below 40 K. The fact that the intercept of the straight line is not exactly at $T_0=10$ K is of no concern, as any other relation mechanism does add to the rate T_1^{-1}, shifting the line vertically.

To account quantitatively for the size of this relaxation, one must assume that only sufficiently fast relaxing nuclei are seen. The others, whose spectrum is not motionally narrowed, are lost. Then $[D]_f$ is obtained from a calculation similar to Eq. (19), but where the upper limit of integration is replaced by $\tau_{\text{eff}}=1/2\pi\nu_{\text{eff}}$, where ν_{eff} is the frequency above which motional narrowing is effective. From the slope in Fig. 10, one finds $\nu_{\text{eff}}=11\times2\nu_L$. The prefactor appears large, but it is not unreasonable when one considers in more detail the likely physical origin of the distribution $g(\tau,T)$ obtained from dielectric relaxation. On one hand, there is a spatial distribution of regions with different relaxation properties; on the other, each region and thus each nucleus is likely to experience a distribution of correlation times. It is the latter that could easily produce the above prefactor. It should be noted that $\nu_c=\nu_{\text{eff}}$ at $T=38.7$ K, so that the crossover from the fast to near-resonant regime occurs at that temperature.

The excellent fits of Figs. 9 and 10 have the great merit of making contact with an energy distribution derived from another measurement. This distribution, being temperature independent, might be difficult to reconcile with the independent-cluster model in which the correlation length, and thus the cluster activation energy, are expected to increase with decreasing temperature.[17] An alternate spin-glass model based on localization theory was elaborated on recently.[20] In this model, the glass formation is related to the temporary freezing of "localized" modes in the Anderson-localization sense.[20] Here, these modes could simply be proton motions on correlated strings of mostly H_2PO_4 Slater configurations. The freezing of the NH_4 groups, which already starts near 100 K, can block randomly the movement of some acid protons, since the ammonia protons also bind to oxygen sites on the PO_4 tetrahedra. If the energy distribution results from this random blocking, it can be essentially temperature independent. Incidentally, the excellent randomicity of the doping was recently confirmed in diffuse x-ray scattering experiments.[6] As a given Rb nucleus is under the influence of a great many of these modes, each Rb experiences a broad distribution of correlation times in this model in agreement with the above discussion of ν_{eff}.

The Vogel-Fulcher temperature simply corresponds to the mobility edge of the localization problem.[20] If one identifies T_0 with T_G of the Edwards-Anderson model,[16] the power-law singularity of T_1^{-1} shown in Fig. 10 is in agreement with a diverging χ_{EA}. The difference from the usual ferroelectric situation (inset of Fig. 4) is then simply that the KD_2PO_4 measurement is in the fast-motion regime, so that T_1 decreases at T_c, whereas the glass measurement is in another regime, causing a near divergence at T_0.

V. SUMMARY AND CONCLUSIONS

To summarize, both proton and ^{87}Rb spin-lattice relaxation times have been measured in $Rb_{1-x}(NH_4)_xH_2PO_4$ with $x=0.35$. The proton T_1 is dominated by slow NH_4 reorientations and is consistent with freezing below ~ 100 K. The Rb T_1 and line shape exhibit unusual features definitely related to a broad distribution of relation times and to an unusually large slowing down of the proton intrabond (O—H $\cdots$ O) motion below ~ 40 K. The qualitative explanation of the Rb T_1 is so far model dependent, and several pictures have been proposed above. In the independent-cluster model, with an Arrhenius relation between cluster relaxation and activation energy, a strongly-temperature-dependent distribution of activation energies is found (Fig. 7). In the Vogel-Fulcher model, on the contrary, the necessary distribution of activation energies is temperature independent between 100 and 10 K (Fig. 8). The parameters derived from the NMR results with the latter model make excellent contact with independent ^{87}Rb EFG tensor data in RbH_2PO_4 on one hand,[15] and with dielectric data on the other.[7]

In closing, we emphasize once more that the Rb T_1 data show a continuous slowing down of the cluster dynamics over the entire temperature range investigated. The slowing down of the proton intrabond motion is much more pronounced and orders of magnitude larger than in other KH_2PO_4-type crystals, where τ_c is only between 10^{-12} and 10^{-11} sec. The NH_4 reorientations, which freeze out at those very low temperatures, are not expected to play a direct role in the dynamics below ~ 30 K. As discussed in a preceding subsection, the crucial role of NH_4 in the formation of the glass might be in the condensation of frozen networks delimiting the fluctuating paraelectric units. This process might start as early as ~ 100 K.

ACKNOWLEDGMENT

This research was supported in part by the Swiss National Science Foundation.

*Present address: J. Stefan Institute, E. Kardelj University of Ljubljana, 61001 Ljubljana, Yugoslavia.

[1]For recent reviews, see articles by J. A. Mydosh, K. Binder, W. Kinzel, G. Parisi, and G. Toulouse, in *Disordered Systems and Localization*, edited by C. Castellani, C. Di Castro, and L. Peliti (Springer, Berlin, 1981). See also K. H. Fisher, Phys. Status Solidi B **116**, 357 (1983).

[2]Eric Courtens, J. Phys. (Paris) Lett. **43**, L199 (1982).

[3]Eric Courtens, Helv. Phys. Acta **56**, 705 (1983).

[4]P. Prelovšek and R. Blinc, J. Phys. C **15**, L985 (1982).

[5]J. C. Slater, J. Chem. Phys. **9**, 16 (1941).

[6]E. Courtens, T. F. Rosenbaum, S. E. Nagler, and P. M. Horn, Phys. Rev. B **29**, 515 (1984).

[7]Eric Courtens, Phys. Rev. Lett. **52**, 69 (1984).

[8](a) D. J. Genin, D. E. O'Reilly, and Tung Tsang, Phys. Rev. **167**, 445 (1968); (b) S. R. Kasturi and P. R. Moran, *ibid.* B **12**, 1874 (1975).

[9]R. Blinc, G. Lahajnar, A. Levstik, R. Osredkar, and L. A. Shuvalov, Phys. Status Solidi B **65**, 397 (1974).

[10]Specifically, we used Eqs. (A8) and (A16) of Ref. 8(b).

[11]R. Blinc and J. Pirš, J. Chem. Phys. **54**, 1535 (1971).

[12]V. H. Schmidt and E. A. Uehling, Phys. Rev. **126**, 447 (1962).

[13]E. Courtens and M. Baumberger (unpublished).

[14]See, e.g., R. Blinc and B. Žekš, *Soft Modes in Ferroelectrics and Antiferroelectrics* (North-Holland, Amsterdam, 1974).

[15]R. Blinc, D. F. O'Reilly, and E. M. Peterson, Phys. Rev. B **1**, 1953 (1970); R. Blinc, M. Mali, and S. Žumer, J. Chem. Phys. **63**, 2898 (1975).

[16]S. F. Edwards and P. W. Anderson, J. Phys. F **5**, 965 (1975); S. Kirkpatrick and D. Sherrington, Phys. Rev. B **17**, 4384 (1978).

[17]W. Kinzel, Phys. Rev. B **26**, 6303 (1982).

[18]S. Shtrikman and E. P. Wohlfarth, Phys. Lett. **85A**, 467 (1981).

[19]See, e.g., A. Abragam, *The Principles of Nuclear Magnetism* (Oxford University Press, Oxford, 1960).

[20]J. A. Hertz, Phys. Rev. Lett. **51**, 1880 (1983); J. A. Hertz, L. Fleishman, and P. W. Anderson, *ibid.* **43**, 942 (1979).